

Site-Dependent classes for the classification of intertidal sediments

Elsy Ibrahim¹ and Jaak Monbaliu²

¹ *Notre Dame University, Louaize. Department of Civil and Environmental Engineering, Zouk Mosbeh, Lebanon; ebrahim@ndu.edu.lb*

² *University of Leuven, Department of Civil Engineering; jaak.monbaliu@bwk.kuleuven.be*

Abstract. The biophysical properties of intertidal sediments highly affect the stability of an intertidal area. Therefore, the characterization of intertidal sediments according to major biophysical properties is essential to understand this sediment stability. Remote sensing technology has been offering great alternatives to classical field data collection methods, where images give full spatial coverage of the study area instead of a set of distributed sampling locations within the study area that are intended to be representative of it. Various methods have been used to characterize sediment properties using remotely sensed imagery, including the highly popular pixel-based supervised classification. The typically considered biophysical properties are grain-size distribution, organic matter content, moisture content, and chlorophyll *a* content. To carry out a supervised image classification, variable classes have to be specified in advance. In literature, these classes have been selected using various scientific or case-dependent justifications due to the challenging fuzzy nature of sediment properties. For example, the limits between wet and dry or sandy and muddy sediments are not easily defined as hard boundaries. Due to this case-dependent nature of the classification, comparing classified imagery of different study sites or different images of the same site has not been practical. This paper addresses the possibility of finding site-dependent classes, instead of case-dependent classes for the classification of the IJzermonding, an intertidal flat in Belgium. This is carried out using field spectra of two independent field campaigns on the IJzermonding. The possibility of obtaining thresholds for the different properties of this site using unsupervised classification is first investigated. The study shows that possible thresholds could be obtained, and each threshold separates a pair of classes for each property, i.e. 20% for moisture content, 3% for organic matter content, 80mg/m² for chlorophyll *a* content, and 10% for mud content. These obtained thresholds are in the range of thresholds commonly used in literature. When compared to a number of other typically used thresholds, they showed higher classification accuracy.

Keywords. remote sensing, hyperspectral, unsupervised classification, supervised classification, intertidal sediments, IJzermonding.

1. Introduction

The importance of physical and biological characteristics of sediments in determining sediment stability leads to a need for frequent field data collection to successfully monitor an intertidal flat. Yet, on such flats, traditional field sampling is often inefficient or unattainable, and covers the study area via sampling locations that are assumed to be representative. Remote sensing offers a more practical and comprehensive alternative to traditional field sediment characterization and has been utilized to distinguish and quantify sediment properties [1], [2], [3].

Intensive work has been done to enhance both supervised and unsupervised classification procedures for sediment characterization, whereby techniques and algorithms of various ranges of complexity have been developed [4]. Depending on the nature of the study area and the number and type of the pre-defined classes that can be discriminated in a statistically correct manner, supervised classification can vary in difficulty. For example, defining lake and forest classes for landuse classification is relatively simpler than defining the boundary between classes of moisture content in the

sediments, due to the gradual variation in sediment properties on tidal flats. Generally, sediment classes have been determined using case-specific field data or from experience and intuition, whereby the class boundaries for a sediment property were often defined using an ad-hoc procedure to end up with an equivalent number of field samples in each class [5]. Some studies based their choices of classes on their experience and knowledge of the study areas [6], [7], [8] or on erosion shear stress [9]. Some grain size classes were defined by merging commonly used classifications based on ternary plots [10]. Furthermore, some researchers chose the classes such that they were physically meaningful and led to a similar distribution of the field samples for each class [2], [11]. Finally, various images of different study sites were classified using the same classes, which were obtained from on a combined view of all the available field data [12].

This case and site dependency of these classes makes it complicated to compare different classified images of the same area. This leads to difficulties in carrying out a multi-temporal study using classification techniques. Although these classes have led to good classification results, classification accuracy can increase when classes are chosen to reflect changes in spectra with respect to a considered property. In what follows, a methodology is proposed which uses the spectral behavior of the data with respect to variation in a sediment property as a suitable basis for choosing sediment classes of a study site. This is carried out using field spectra and field data accompanied by airborne hyperspectral imagery on one study site. The field spectra and data are used to find adequate classes, and imagery is used to test the suitability of these classes.

2. Study area and data acquisition

The study area is “the IJzermondung”, an intertidal flat located at the outlet of the IJzer river at the Belgian coast (Figure 1). It is a nature reserve that consists of dunes, marshes, and mudflats with a total area of 130 hectares. In 1994, this study site - as part of the IJzer valley - became a part of the EC Special Protection area for birds. In 1999, a restoration project was carried out where buildings, docks, and most constructions were removed. This created larger areas of mudflats and marshes, where the stability of these mudflats assures the nature reserve’s well-being.

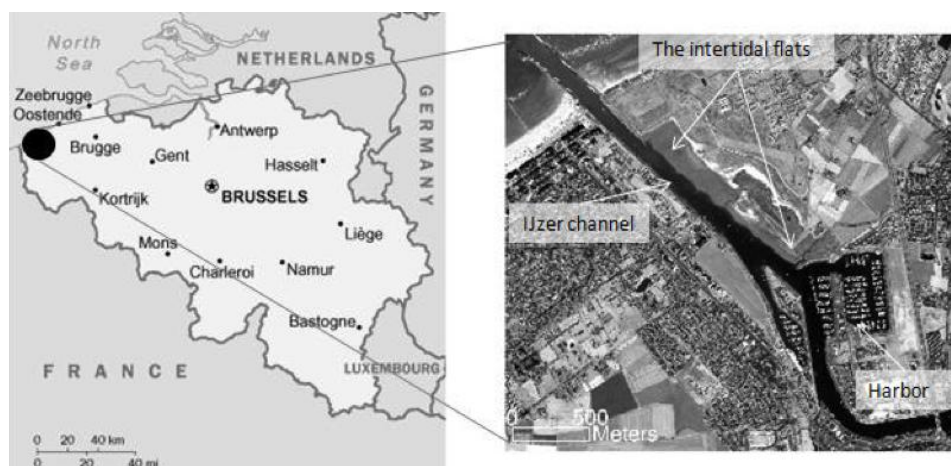


Figure 1. The location of the IJzermondung

3. Flight campaigns

On the 17th of June 2005, and the 12th of June 2007 images of the IJzermending were acquired in cloud-free conditions by means of the Airborne Hyperspectral Sensor (AHS).

4. Field campaigns

Field campaigns were carried out on the intertidal flat, at low tide, to accompany the acquired images. For each campaign, sampling sites were chosen such that the highest diversity in sediment properties was included. The coordinates of the sampled sites were determined by a Differential Global Positioning System (DGPS) and surface reflectance measured by an Analytical Spectral Device (ASD) spectrometer. The ASD spectrometer records the reflectance in the visible, near-infrared and shortwave infrared region of the spectrum with a spectral resolution of 3 nm for the region 350–1000 nm and 10 nm for the 1000–2500 nm region.

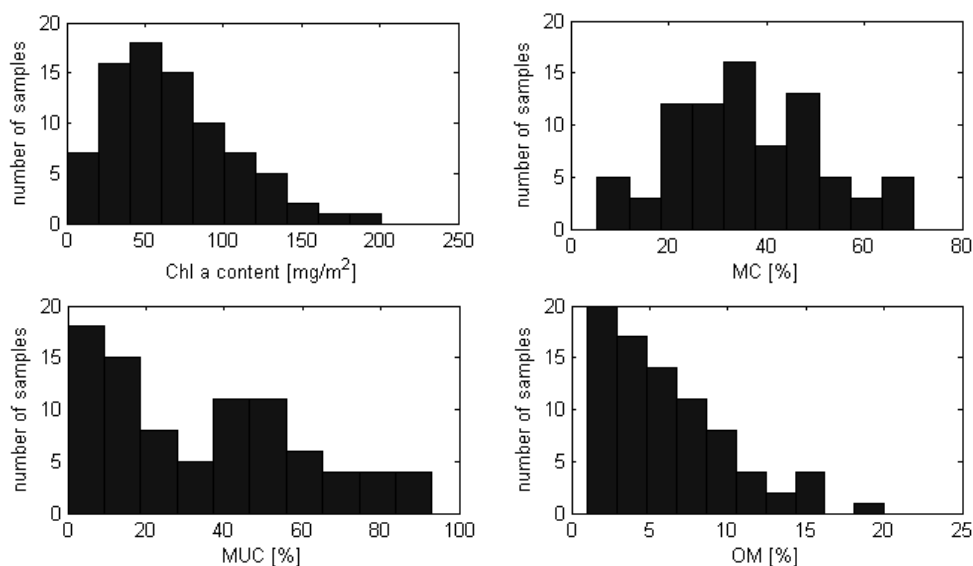


Figure 2. The distribution of sediment properties of 2005 samples

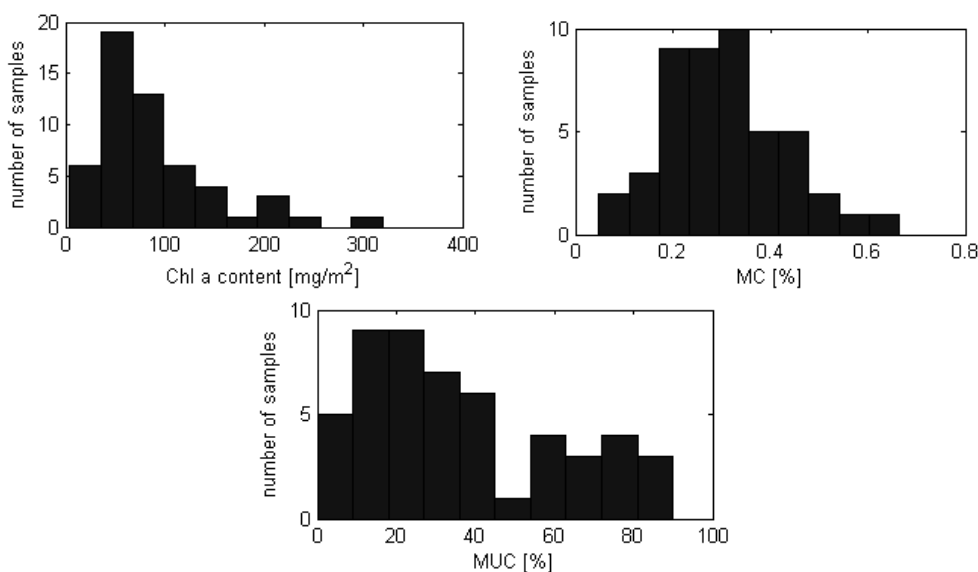


Figure 2. The distribution of sediment properties of 2007 samples

In 2005, 28 sites were sampled four days before the flight (Figure 2). To account for the variability within one pixel, two or three replicate samples, within 2 meters, from the site were taken leading to 80 measurements in total. Surface sediment was collected and analyzed for chlorophyll a content (chl a), moisture content (MC), organic matter content (OM), and grain size distribution. In 2007, the field campaign was carried out 8 days after the overflight. Field sampling at 63 sites was performed, and only one sample was taken at each site. Samples were analyzed for MC, grain size distribution, and chl a content. The sediment properties distributions of these samples corresponding to these two properties are shown in are shown in Figure 2, and Figure 3 where mud content refers to refers to cohesive particles smaller than $63\mu\text{m}$.

5. Methodology

5.1. Overview:

It is not common to have reflectance from imagery correspond to the exact time of field sampling. Therefore, due to the high temporal variability of the sediment, there is always an uncertainty in linking field data to image spectra. For this reason, the ASD spectra are used for this analysis, as they were collected simultaneously with the field samples, and thus offer a great opportunity to minimize uncertainties in linking reflectance spectra to the sampled locations.

The field spectra are first classified in an unsupervised manner. Then, the sediment properties corresponding to each cluster are investigated. On this basis, thresholds for sediment classes are chosen. In a last step, the images accompanying the field spectra are classified in a supervised manner using the thresholds set in the previous step.

Through classification, the affiliation of feature vectors to specific groups are assigned by conditional probabilities, which represent the probability of an unknown feature vector to belong to a class. These are referred to as a posteriori probabilities. Depending on the classification approach, a classifier computes either the maximum of these probabilities or the maximum of a defined function of them. An unknown feature vector is then assigned to belong to the group corresponding to this maximum.

5.2. Unsupervised classification:

The first step in unsupervised classification is finding structure in a collection of unlabeled data using clustering techniques. Clustering partitions a data set into a defined number of clusters for which the a posteriori probabilities are not known. In this paper, the data sets are ASD spectra of each field campaign. The Mixture of Gaussians approach is used for the classification using the procedure described by [13] and [14].

Dimensionality can be a critical factor for image classification, whereby a successful reduction of the number of dimensions can lead to an increase in computational efficiency and classification accuracy [15], [16], [2]. For the unsupervised classification, the high dimensionality of the field spectra is reduced by spectral resampling to the spectral resolution of the airborne image corresponding to each considered field campaign.

5.3. Linking field samples to unsupervised classification:

The second step in the process is to identify the distribution of the field samples in the resulting clusters. The field samples are grouped according to their clusters of affiliation. Then, they are addressed regarding each considered sediment property, i.e. moisture content, organic matter content, chl a content, and mud content. Spectrally significant thresholds per property can be then chosen.

These thresholds can indicate the spectrally distinguishable classes for each individual sediment property.

5.4. Supervised classification:

The field data used for classification are divided into the property classes according to the thresholds found as explained above. A part of the data set is used to train the classifier. Then, the supervised classifier predicts the class of each of the remaining unknown pixels in the image. In the validation phase, using the remaining data, the ability of a classifier to correctly classify the data can be assessed. In this work, for illustration purposes, Support Vector Machines (SVM) was used for the classification [17], [18]. It is a binary classifier that has been widely used for the classification of hyperspectral data. The classification accuracy was then measured using the kappa statistic (K), which describes the proportion of correctly classified field samples after random agreements are removed [19].

6. Results

6.1. Unsupervised classification of the data:

Each ASD data set of each campaign is considered. Each data set is classified in an unsupervised manner using the MG approach, leading to three clusters for 2005 and four clusters for 2007 data.

6.2. The distribution of field data within the resulting clusters:

Figure 4 and Figure 5 show the distribution of properties within the clusters of field spectra.

- MC shows the clearest distinction between around 20%. Thus, MC is considered “low” when below 20% and “high” otherwise.
- OM shows distinction in reflectance when a threshold is set between 2% and 4% organic matter content. 3% is chosen as the threshold: “low OM” for organic matter below 3% and “high OM” otherwise.
- Chl *a* groups are not well distinguished in the 2005 cluster analysis. Yet, in the 2007 data sets, a possible threshold can be considered around 80mg/m². Thus, chl *a* content is considered “low” when below 80mg/m² and “high” otherwise.
- In the 2005 data set, possible patterns can be considered around 10% mud content. Thus, MUC is considered “low” when below 10% and “high” otherwise.

6.3. Supervised classification of hyperspectral imagery:

For illustration purposes, the airborne hyperspectral image acquired by AHS in 2005 is classified using the classes achieved from the unsupervised classification. Furthermore, the classification accuracy is compared to other common thresholds used in literature. Table 1 shows the classification accuracy in terms of kappa statistic. Figure 6, Figure 7, Figure 8, and Figure 9 show the classification results of the 2005 image with respect to each sediment property using the obtained thresholds.

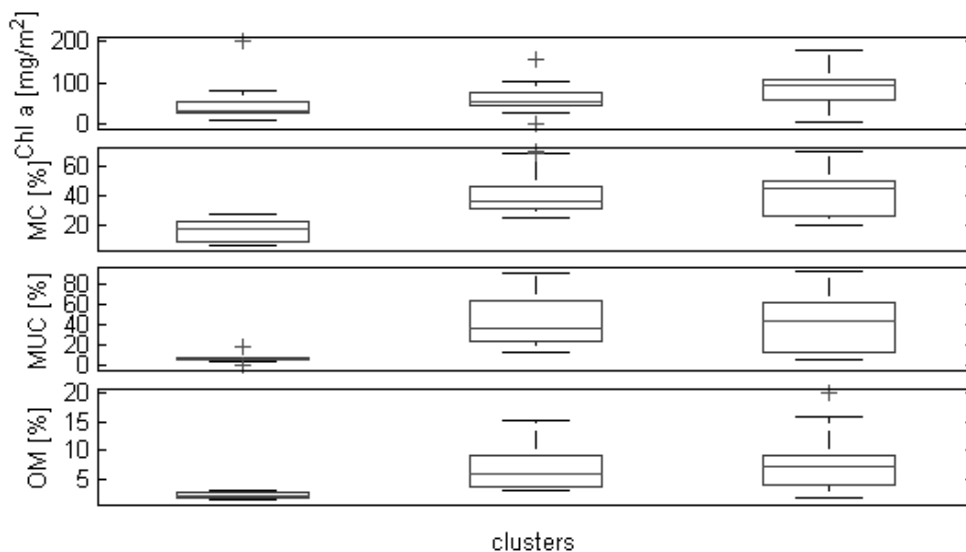


Figure 3. Distribution of sediment properties within the clusters of 2005 field spectra

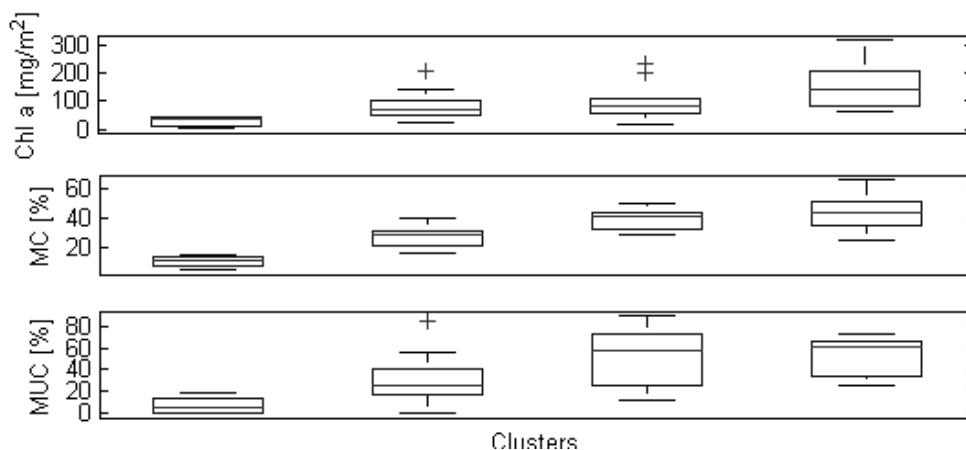


Figure 4. Distribution of sediment properties within the clusters of 2007 field spectra

Table 1. Classification accuracy using the thresholds achieved from the unsupervised classification (in bold) and other typically used thresholds.

Property	Threshold	Kappa
MC	20%	0.95
	25%	0.88
	30%	0.85
OM	3%	0.88
	4%	0.82
	10%	0.75
Chl a	40 mg/m ²	0.32
	80mg/m²	1.0
MUC	10%	0.83
	30%	0.7

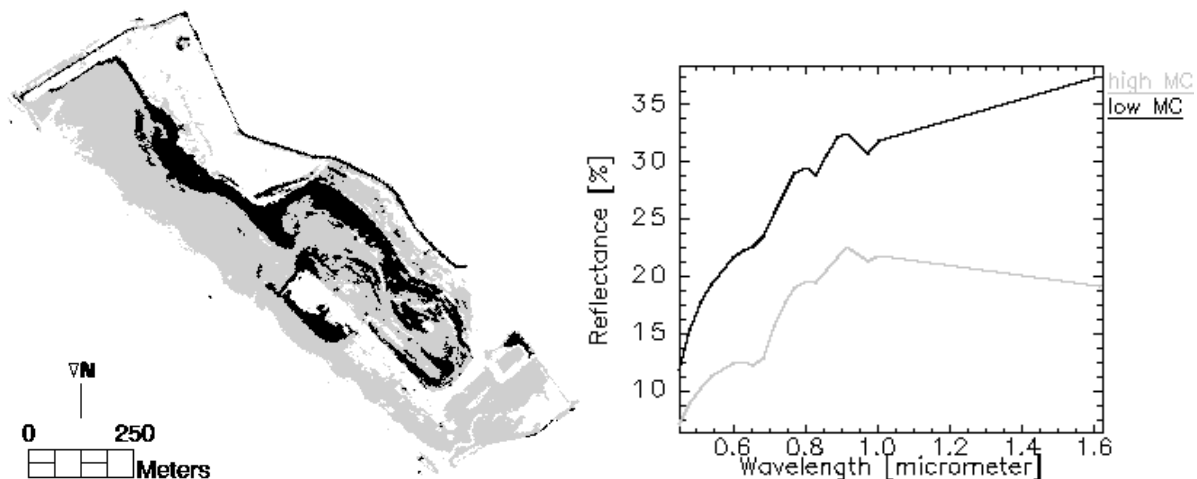


Figure 5. MC classification of AHS 2005 of the IJzermondig using 20% threshold (left: classified image, right: mean spectrum for each class)

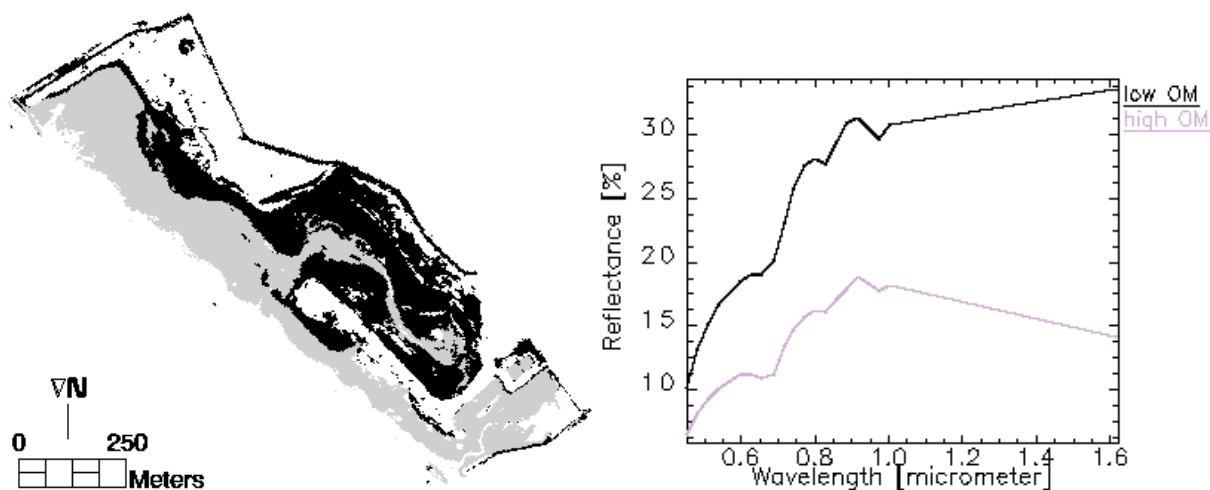


Figure 6. OM classification of AHS 2005 of the IJzermondig using 3% threshold (left: classified image, right: mean spectrum for each class)

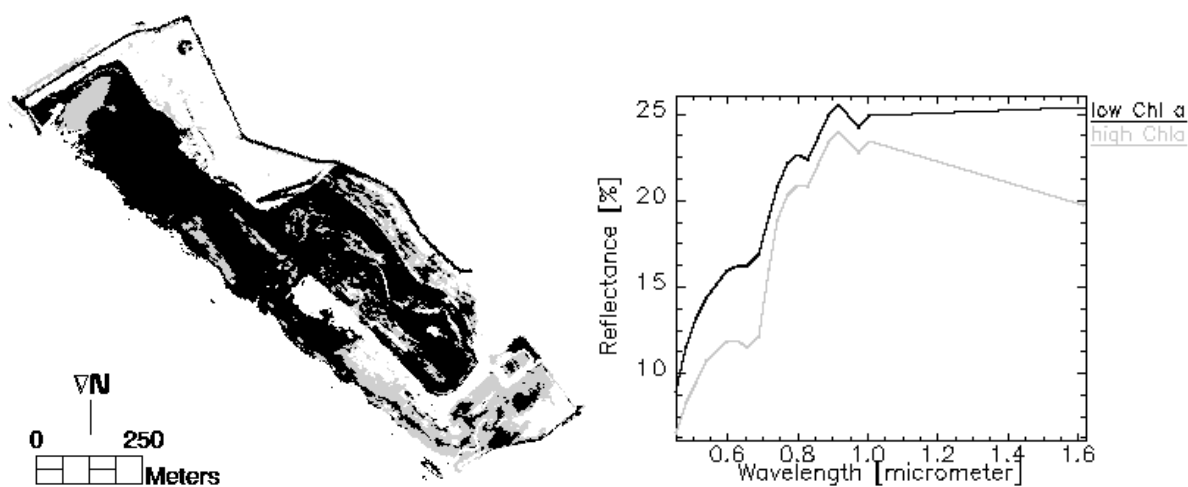


Figure 7. Chl a classification of AHS 2005 of the IJzermondig using 80mg/m2 threshold (left: classified image, right: mean spectrum for each class)

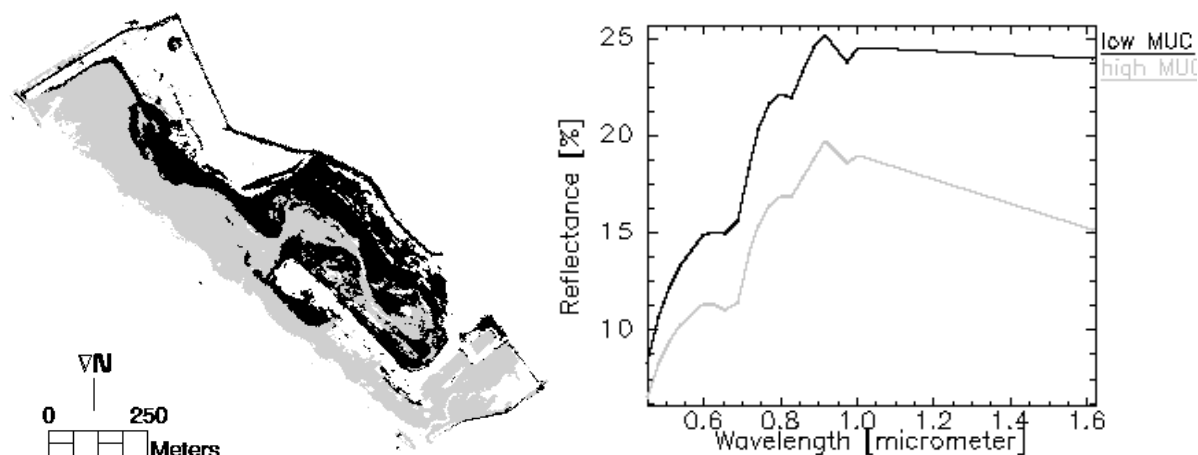


Figure 8. MUC classification of AHS 2005 of the IJzermonding using 10% threshold (left: classified image, right: mean spectrum for each class)

7. Conclusions

The study suggests a method to choose classes for intertidal sediment properties based on the spectral behavior of image reflectance with respect to variation in a sediment property. This is carried out using field spectra and field data accompanied by airborne hyperspectral imagery on one study site. The field spectra and data are used to find adequate classes, and imagery is used to test the suitability of these classes.

The study shows that possible thresholds could be obtained using the suggested methodology. These thresholds are to separate a pair of classes for each property, i.e. 20% for moisture content, 3% for organic matter content, 80mg/m² for chlorophyll a content, and 10% for mud content. These obtained thresholds are in the range of thresholds commonly used in literature. When compared to a number of other typically used thresholds, they show higher classification accuracy.

The study shows the potential of obtaining standard classes for the IJzermonding. Yet, other field campaigns and imagery are to be used in order to assess the applicability of these thresholds as the flat evolves. Furthermore, a similar study should be carried out on other intertidal flats to compare the obtained thresholds to those of the IJzermonding.

Acknowledgements

The research presented in this paper is funded by the Belgian Science Policy Office in the frame of the STEREO II programme, project SR/00/109 - ALGASED (remote sensing for characterization of inter-tidal sediments and microphytobenthic algae).

Partial support of this research is by the FP7 project THESEUS (Innovative technologies for safer European coasts in a changing climate).

The field and flight campaigns were supported by the Belgian Science Policy in the framework of the STEREO programme, project SR/00/043, 072.

References

- [1] Rainey, M., Tyler, A., Gilvear, D., Bryant, R., and McDonald, P., "Mapping intertidal estuarine sediment grain size distributions through airborne remote sensing," *Remote Sensing of Environment*, vol. 86, pp. 480–490, 2003.

- [2] Deronde, B., Kempeneers, P., and Forster, R., "Imaging spectroscopy as a tool to study sediment characteristics on a tidal sandbank in the Westerschelde," *Estuarine, Coastal and Shelf Science*, vol. 69, pp. 580–590, 2006.
- [3] Adam, S., "Bio-physical characterization of sediment stability indicators for mudflats using remote sensing," Ph.D. dissertation, Katholieke Universiteit Leuven, Belgium, 2009.
- [4] Lillesand, T. and R. Kiefer, *Remote sensing and image interpretation*. John Wiley & Sons, Inc, 2000.
- [5] Defew, E., Tolhurst, T., and Paterson, D., "Site-specific features influence sediment stability of intertidal flats," *Hydrology and Earth System Sciences*, vol. 6, pp. 971–982, 2002.
- [6] Yates, M., Jones, A., McGrorty, S., and Goss-Custard, J., "The use of satellite imagery to determine the distribution of intertidal surface sediments of the Wash, England," *Estuarine, Coastal and Shelf Science*, vol. 36, pp. 333–344, 1993.
- [7] Thomson, A., Fuller, R., Yates, M., Brown, S., Cox, R., and Wadsworth, R., "The use of airborne remote sensing for extensive mapping of intertidal sediments and saltmarshes in eastern England," *International Journal of Remote Sensing*, vol. 24, pp. 2717 – 2737, 2003.
- [8] Smith, G. M., Thomson, A. G., Möller, I., and Kromkamp, J. C., "Using hyperspectral imaging for the assessment of mudflat surface stability," *Journal of Coastal Research*, vol. 20, pp. 1165 – 1175, 2004.
- [9] Hakvoort, J. H. M., Heineke, M., Heymann, K., Kuhl, H., Riethmüller, R., and Witte, G., "Optical remote sensing of microphytobenthic biomass: a method to monitor tidal flat erodibility," *Senckenbergiana maritima*, vol. 29, pp. 77–85, 1998.
- [10] Flemming, B. W., "A revised textural classification of gravel-free muddy sediments on the basis of ternary diagrams," *Continental Shelf Research*, vol. 20, pp. 1125–1137, 2000.
- [11] Adam, S., Vitse, I., Johannsen, C., and Monbaliu, J., "Sediment type unsupervised classification of the Molenplaat, Westerschelde estuary, the Netherlands," *EARSeL eProceedings*, vol. 5, pp. 146–160, 2006.
- [12] Ibrahim, E. and Monbaliu, J., "Supervised classification of hyperspectral images of algased," the ALGASED project, Report, 2009.
- [13] Biernacki, C., Celeux, G., Govaert, G., and Longrogniet, F., "Model-based cluster and discriminant analysis with the MIXMOD software," *Computational Statistics & Data Analysis*, vol. 51, pp. 587–600, 2006.
- [14] Ibrahim, E., Adam, S., vanderWal, D., DeWever, Sabbe, A., K., Forster, R., and Monbaliu, J., "Assessment of unsupervised classification techniques for intertidal sediments," *EARSeL eProceedings*, vol. 8(2), pp. 158–179, 2009.
- [15] Jain, A. and Zongker, D., "Feature selection: evaluation, application, and small sample performance," *IEEE Transactions on Pattern Analysis and Machine Intelligence*, vol. 19, pp. 153–158, 1997.
- [16] Forman, G., "A pitfall and solution in multi-class feature selection for text classification," in *Proceedings of the 21st International Conference on Machine Learning (ICML 04)*, 2004.
- [17] Vapnick, V. N., *Statistical learning theory*. John Wiley and Sons Inc., 1998.
- [18] Dalponte, M., Bruzzone, L., Vescovo, L., and Gianelle, D., "The role of spectral resolution and classifier complexity in the analysis of hyperspectral images of forest areas," *Remote Sensing of Environment*, vol. 113, pp. 2345–2355, 2009.
- [19] Rosenfield, G. H. and Fitzpatrick-Lins, K., "A coefficient of agreement as a measure of thematic classification accuracy," *Photogrammetric Engineering & Remote Sensing*, vol. 52, pp. 223–227, 1986.

